

Validation Testing of Multiple IMUs as Sensors of Joint Angles

Ryan Casey

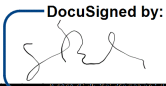
Georgia Institute of Technology

Dr. Anirban Mazumdar - Mentor

Signed:  _____

Date: 12/09/2021

Dr. Essy Behravesh - 2nd reader

Signed:  _____
A3317F272CB5458...

Date: 12/10/2021 | 2:30 PM EST

Table of Contents

| | |
|------------------------------|----------------|
| Introduction | 3 - 4 |
| Literature Review | 4 - 6 |
| Materials and Methods | 7 - 12 |
| Results | 12 - 16 |
| Discussion | 16 - 20 |
| Conclusion | 20 |
| References | 20 - 21 |

Introduction

Gathering joint angles is a particular challenge in quantifying biomechanics. It is usually done with very expensive, very specific equipment such as motion capture systems. Because of this, there is limited accessibility to measuring joint angles, and limited capability for robots such as exoskeletons that may need to rely on real-time joint angle measurement in real time to perform properly. Using wearable sensors to measure joint angles would significantly reduce the cost of measuring joint angles relative to motion capture systems, which would greatly improve the accessibility of measuring joint angles. Furthermore, wearable sensors would be possible to incorporate into the design of an exoskeleton. The focus of this research project, then, was to find a way to use wearable sensors to quantify joint angles in real-time.

Many types of sensors were considered for this task, such as a piezoelectric strain sensor, which has been found to be an effective sensor at measuring angles¹. However, due to practicality, feasibility, and access to materials, IMUs (internal measurement units) were chosen as the wearable sensor to investigate.

IMUs can measure a variety of different factors including speed, acceleration, direction, angular rate, and specific force⁸. They do this by combining measurements from an accelerometer, gyroscope, and magnetometer. The accelerometer is capable of returning its velocity, as well as roll and pitch, the gyroscope can return rotation and rotational rates, and the magnetometer serves as the tool for gravitational force measurement as well as yaw. These three components complement each other very well and allow for somewhat of an internal validation of the angular measurements. This is why IMUs were chosen as the sensor for angular measurements.

The particular IMUs that were originally going to be used for this experiment were Adafruit™'s BNO055 series, due to their relative abundance and cheap cost. However, upon beginning to work with them, it was noted that angular measurements tend to “drift” the longer these IMUs are sending data, even if the actual angle of the device is not changing. Because of this, a far more expensive yet reliable IMU was chosen for validation testing as well: Microstrain™'s IMU. The BNO055 IMU utilizes a MEMS accelerometer and a low-performance gyroscope, whereas Microstrain™'s IMU incorporates a high-performance triaxial accelerometer, a high-performance triaxial gyroscope, and far more on-board filtering than the BNO055 IMU. However, rather than remove the BNO IMU from validation testing, the decision was made to investigate both IMUs simultaneously.

Adding a second IMU to the experiment made the focus of this research twofold. The first goal of this research was to test each IMU's absolute performance, and the second was to compare the performance of the two IMUs. In order to do this, an experiment was designed in which a subject wore these IMUs while performing various movements and being observed by a motion capture system, which acted as the ground truth metric that the IMU readings were compared against. Both low force movements (walking) and high force movements (sprinting) were done to test the IMUs under a variety of contexts.

Literature Review

There are several ways of synthesizing a limb wearable, with most of the variance between designs coming from the difference in sensors used. One study was able to create a very accurate wearable by fabricating their own strain sensors¹. It worked by having a piezoelectric strain sensor placed across the knee, which would have a change in impedance with deformation. The angle of

the knee could then be determined by the measured change in impedance. This approach was very unique, however it turned out to be infeasible due to limited resources and capabilities. The more common approach is to use internal measurement units (IMUs) as the sensor to determine joint angles. An IMU can return its absolute accelerations and rotations in 3 dimensions, so by placing two IMUs across a joint, their relative change in angle is equal to the angle of the joint^{2,3}.

For limb wearables, dealing with the arm in particular is challenging because of the degrees of freedom of the shoulder. Most advanced models treat the shoulder as 3 degrees of freedom, but it actually has more if you consider that the shoulder can move around within the socket as well. One study resolved this issue by finding that the shift within the shoulder joint is relative to the angle of the arm, so a sliding joint on the shoulder should deal with this issue³. This is something that would be very complicated to implement, so for the purposes of this experiment, the arms were avoided as members of the body to measure angles with, and hip flexion was investigated instead.

A study done at the University of Michigan investigated IMUs as a sensor to measure lower body angles via a similar methodology as this paper; Movements were done in a motion capture space and motion capture data was compared against IMU readings¹⁰. This particular study, however, looked at OPAL IMUs and knee angles, rather than BNO IMUs, Microstrain IMUs, and hip angles. This study found that the OPAL IMUs had an RMSE of 8.4 degrees for flexion, 4.9 degrees for adduction, and 3.9 degrees for rotation.

One of the potential capabilities of IMUs as a sensor is that they may be capable of aiding exoskeletons by returning joint angles in real time. Exoskeletons can be either active (powered by something) or passive. Dealing with the easier of the two first, passive exoskeletons usually work by having a heavy weight offset the desired load that someone is lifting, and this allows the torque about the joint of interest to be lessened. There are also several other

methods that passive exoskeletons employ to achieve muscle activity reduction. One recurring theme is the use of some sort of material to store energy throughout the concentric phase of a lift (the descent) and release during the eccentric phase (the ascent). By doing this, a passive exoskeleton can aid the lift even more, and achieve greater results. One way to achieve this is to use a carbon fiber material⁴ and another way is to use something similar to a spring⁵. Unlike passive exoskeletons, active exoskeletons are a more expensive and more effective alternative to passive ones. Some are very strong and can reduce EMG activation of the wearer by up to 80%⁶, but these are also very expensive. On the other hand, some are made out of soft and comfortable material, and are only meant to slightly facilitate normal human motions.

One such design is the autonomous multi-joint soft exosuit⁷. This exoskeleton looked at leg muscle and lower back muscle activation. The autonomous multi-joint soft exosuit worked by having a sensor read heel strike upon every step, and actuate about the knee and hips accordingly to facilitate walking. The study found that the exoskeleton was able to reduce metabolic cost of the user by 14.4% from normal, and by 22.3% if they were to be wearing the exoskeleton without it turned on. This sort of pairing between human motion and actuation could also potentially be facilitated by IMU readings of joint angles, which is the basis of this thesis.

Materials and Methods

1 Experimental design:

1.1 Overview:

The goal of this experiment was to use a BNO IMU and Microstrain IMU inside of a state of the art motion capture facility and simultaneously get angular data from both IMUs and the motion capture space to be able to compare the two. Hip flexion of the right leg was chosen as the angle being compared between all three devices.

The motion capture space is equipped with motion cameras which can very accurately measure joint angles over time. Using the space allowed the measurements of joint angles from the wearable device to be validated by a reliable and accurate method of measurement.

1.2 Experiment One:

The subject was asked to stand motionless for 30 seconds. This was performed for a single 5-minute trial. The purpose of this experiment was to serve as a control and to test if there was any “drift” in the angular readings of the IMUs over time. This experiment was meant to inform data processing for Experiment Two. If a significant amount of “drift” was qualitatively observed in either IMU, then data processing for Experiment Two would be done with and without correcting this “drift”.

1.3 Experiment Two:

The subject was asked to walk on a treadmill for 5 minutes at 4 different speeds: 1.75 m/s, 1.5 m/s, 1.25 m/s, and 1 m/s. Each trial was performed just once.

1.4 Experiment Three:

The subject was asked to emulate the motion of breaking into a sprint for about 30 feet from a complete stand-still. This was done at irregular intervals, so the subject had to react to call outs, and could not predict when they would have to break into a sprint. Due to there only being three consecutive pairs of force plates in the motion capture space, only about 6 lateral feet of force data can be

captured for each trial, so 4 different start points were used to capture force data at different points in the subject's motion.

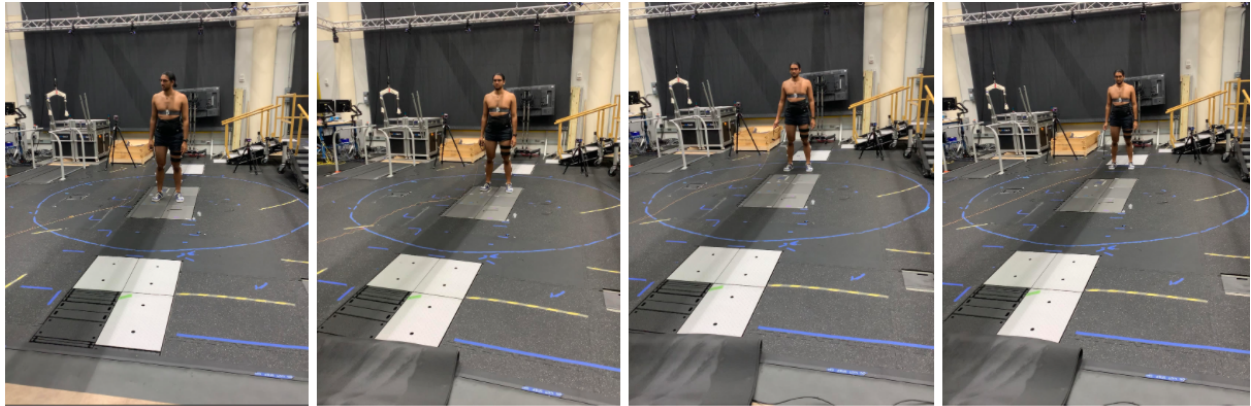


Figure 1. Sprinting trials differing start points relative to force plates.

Moreover, at each start point, trials were performed with a lead left leg and lead right leg. Each trial variation was performed 5 times for a total of 40 sprinting trials. A labelling system was developed for the trials. The first letter of a trial corresponds to where the subject started their motion. C denotes the center of the force plates, B denotes 2 feet back from C, B1 denotes 4 feet back from C, and B2 denotes 6 feet back from C. The second letter of each trial corresponds to which leg the subject initially pushed off of. L denotes left and R denotes right. Lastly, the number denotes which trial it was in chronological order. Examples of individual sprinting trial names would be 'B1_R_3' or 'C_L_5'.

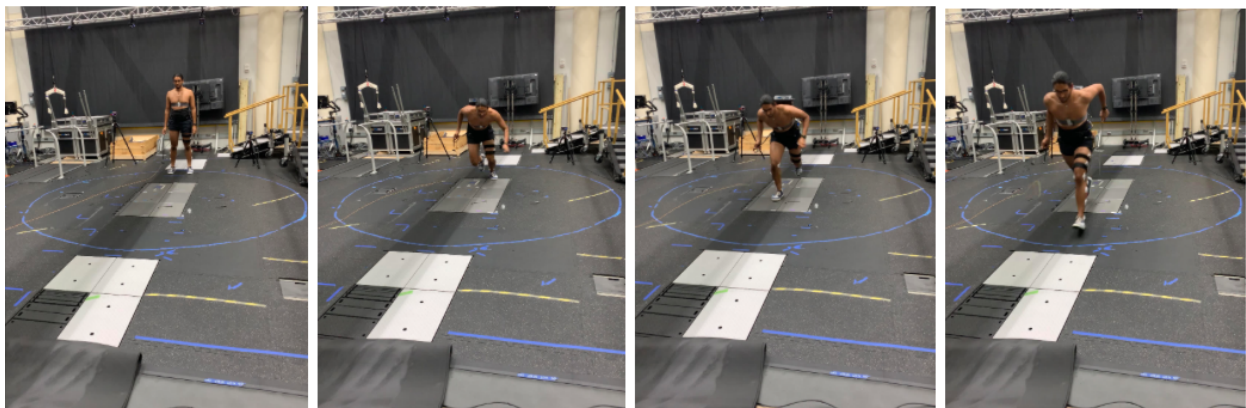


Figure 2. Example of Sprinting trial. Trial 'B1_R_3'.

2 Population:

All of the testing was done on 1 male subject who was 6 foot 2 inches tall and 200 pounds at the time of testing. This study was performed under an IRB Protocol approved by the Georgia Institute of Technology Institutional Review Board (IRB H18363). After the participant gave written informed consent, they were fitted with reflective markers and placed in the Vicon space where their movements could be studied.

3 Motion Capture:

Motion capture cameras were used to quantify the motions performed by the subjects. The “plug-in-gait” marker set model was the marker set used on the subjects (shown below).

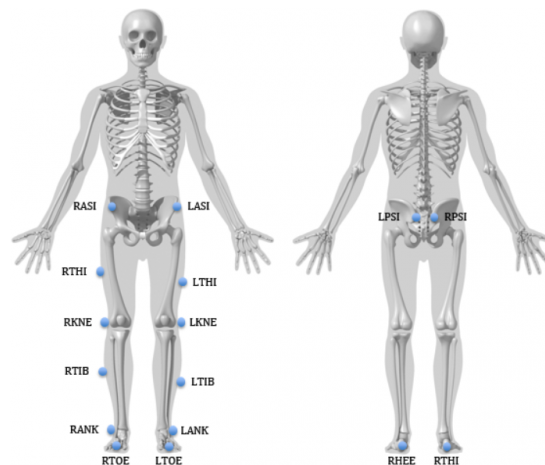


Figure 3. Plug-in-Gait Marker Set

4 IMU Set Up:

A Microstrain IMU and a BNO IMU were fixed into a plastic casing. This plastic casing was then secured to the subject's right leg via velcro straps.

The subject was also wearing a device with a microprocessor with accompanying electronics for a hip exoskeleton. Inside were motor controllers, relays, a battery, raspberry pi, and assorted electronics for the system. For this experiment of IMU validation, only the raspberry pi and battery within the device were being used, but the whole device was worn to more accurately emulate a subject who was wearing an exoskeleton.

The raspberry pi was connected to and received data from both IMUs. This data was transferred from the raspberry pi to a computer between trials via a USB flash drive.

Lastly, a sync pin was connected from the Vicon system to the raspberry pi that sent a high signal every time a Vicon trial had begun recording. This enabled a known start point in time of data collection between the Vicon system and the IMUs.

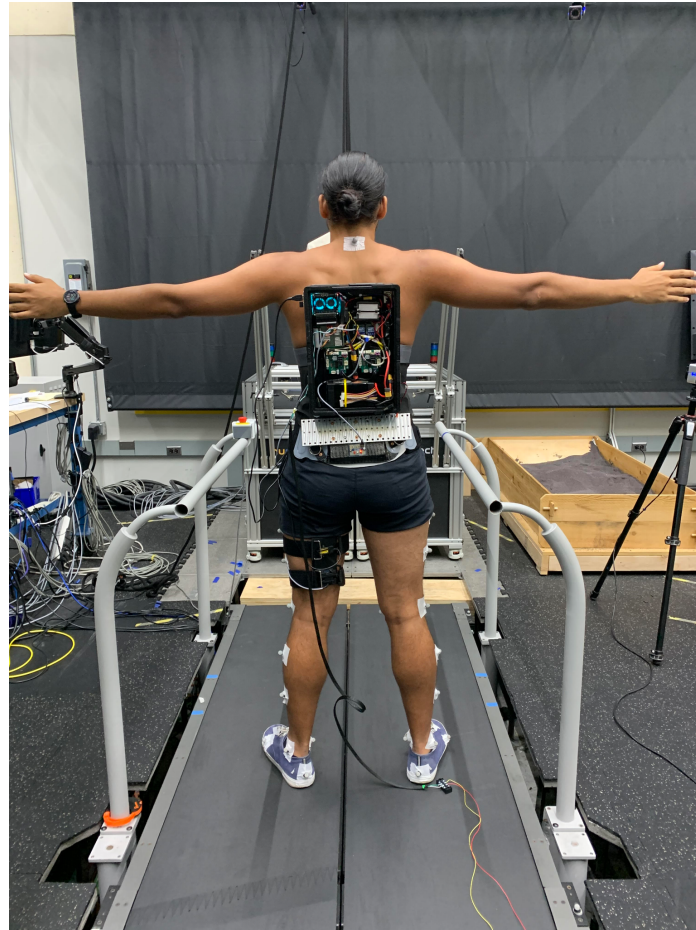


Figure 4. Plastic casing with IMUs (right leg). Device with raspberry pi (back).
Sync pin (floor).

5 Data Processing:

5.1 Motion Capture Validation:

Motion capture data was manually processed using Vicon Nexus version 2.12. This manual processing included checking all of the markers for every trial, and making sure that markers hadn't disappeared or flipped for a few frames, and that their labelling was correct. Switched markers were manually switched

back, and missing markers were approximated for the frames that they were missing using Vicon's "Rigid Body Fill" feature.

5.2 Angular Data:

Once all of the marker set data had been manually processed, OpenSim version 4.3, a motion analysis software, was used to convert this raw data into angular data of the right hip joint.

6 Statistical analysis:

For the walking trials, only RMSE (root mean squared error) of the angles between the Microstrain IMU and Motion Capture Data, and the BNO IMU and Motion Capture Data were calculated. A paired-sample t-test was then done between the RMSE values of the BNO IMU and Microstrain IMU for every trial.

For the sprinting trials, phase was easily determinable, so phase between the IMUs and Motion Capture Data was calculated. This also allowed for a "phase shifted RMSE" to be calculated along with a regular RMSE. The "phase shifted RMSE" corrected any lag between the Motion Capture Data and the IMU readings before calculating RMSE. Paired-sample t-tests were then done between the BNO IMU results and Microstrain IMU for all three metrics: RMSE, phase shift, and shifted RMSE. A paired-sample t-test was done on the overall results from every sprinting trial grouped together, and paired-sample t-tests were also done for every subgroup of sprinting trials.

Trials where the sync pin malfunctioned had to be thrown out.

Results

Experiment 1:

Drift could not be seen qualitatively in either the BNO IMU or the Microstrain IMU, so “drift corrected” results were not generated for the walking trials (Experiment Two).

Experiment 2:

The RMSE of the BNO IMU data relative to the motion capture data for the 1.75 m/s, 1.5 m/s, 1.25 m/s, and 1.0 m/s trials were 31.98°, 43.89°, 23.44°, and 18.80°, respectively. The RMSE of the Microstrain IMU data relative to the motion capture data for the 1.75 m/s, 1.5 m/s, 1.25 m/s, and 1.0 m/s trials were 24.22°, 37.51°, 23.56°, and 14.01°, respectively.

The overall RMSE of all walking trials combined were 29.53° and 24.82° for the BNO IMU and Microstrain IMU, respectively. The p-value for the t-test between RMSE of each trial was .0717.

Pictured in figure 5 is a comparison of the hip flexion angular readings of the 1.75 m/s trial and 1.0 m/s trial between 10 and 20 seconds. The Microstrain IMU (yellow), BNO IMU (orange), and Motion Capture Cameras (blue), are all shown.

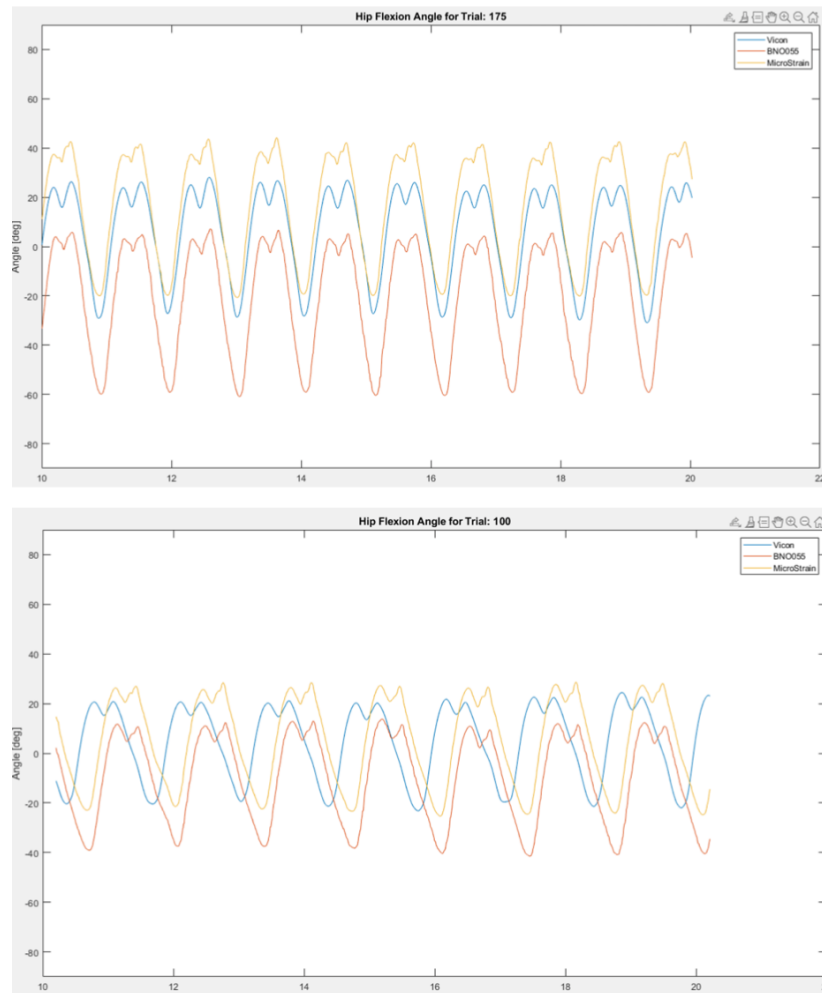


Figure 5. Comparison of data visualization between 1.75 m/s and 1.0 m/s walking trial.

Experiment 3:

The overall mean RMSE between the Microstrain IMU data and motion capture data for all sprinting trials was 13.51° , and the overall mean RMSE between the BNO IMU data and motion capture data for all sprinting trials was 16.48° , with a p-value of $< .0001$.

The overall mean phase between the Microstrain IMU data and motion capture data for all sprinting trials was 0.0284 seconds, and the overall mean phase between the BNO IMU data and motion capture data for all sprinting trials was 0.0489 seconds, with a p-value of $< .0001$.

The overall shifted mean RMSE between the Microstrain IMU data and motion capture data for all sprinting trials was 13.55° , and the overall shifted mean RMSE between the BNO IMU data and motion capture data for all sprinting trials was 15.15° , with a p-value of $.0001$.

The metrics for each subset of sprinting trials and the p-values for the t-tests between the different IMU's results are shown in the tables below.

| | bnoRMSE (degrees) | microRMSE (degrees) | pvalue |
|-------------------|-------------------|---------------------|-----------|
| Sprinting Overall | 16.4823072 | 13.51167681 | $< .0001$ |
| C_L | 10.79629544 | 9.024665899 | 0.0233 |
| C_R | 16.33730981 | 13.08252024 | 0.0251 |
| B_L | 14.41518046 | 10.73167914 | 0.0132 |
| B_R | 21.15598981 | 15.81442202 | 0.0026 |
| B1_L | 15.15296065 | 12.33530215 | 0.0011 |
| B1_R | 18.40973607 | 13.81043481 | 0.0001 |
| B2_L | 17.97278159 | 19.10512468 | 0.2622 |

Figure 6. Table showing RMSE for each subset of sprinting trials.

| | bnophase (s) | microphase (s) | pvalue |
|-------------------|--------------|----------------|---------|
| Sprinting Overall | 0.048929811 | 0.028411108 | < .0001 |
| C_L | 0.015121 | -0.0021412 | 0.0039 |
| C_R | 0.1302874 | 0.1015042 | 0.0002 |
| B_L | 0.0067628 | -0.0071162 | 0.0065 |
| B_R | 0.0862032 | 0.0614126 | 0.0004 |
| B1_L | 0.0085078 | -0.0059088 | 0.0039 |
| B1_R | 0.072916 | 0.0474648 | 0.0018 |
| B2_L | 0.0230566 | 0.006289 | 0.032 |

Figure 7. Table showing phase for each subset of sprinting trials.

| | shifted bnorMSE (degrees) | shifted microRMSE (degrees) | pvalue |
|-------------------|---------------------------|-----------------------------|--------|
| Sprinting Overall | 15.15219566 | 13.55823939 | 0.0001 |
| C_L | 10.35604605 | 9.028795557 | 0.0315 |
| C_R | 16.1950098 | 15.63697199 | 0.542 |
| B_L | 14.31571 | 10.72922533 | 0.0154 |
| B_R | 15.84601721 | 13.84460307 | 0.0301 |
| B1_L | 15.12658817 | 12.4195685 | 0.0163 |
| B1_R | 16.25366774 | 13.840741 | 0.001 |
| B2_L | 17.40698566 | 18.95480622 | 0.1387 |

Figure 8. Table showing shifted RMSE for each subset of sprinting trials.

By the end of this experiment, the sync pin being used stopped firing, making the last few sprinting trials contain unusable data. This is why no metrics are recorded for the B2_R trials.

Discussion

Experiment 2:

There are two general trends among the data; The first is that RMSE decreases as walking speed decreases, and this is no surprise, given that IMUs are known to become less reliable when greater forces are involved, as this interferes with their internal accelerometers. The second trend was that the Microstrain IMUs outperformed the BNO IMUs. This again is of no surprise given that the Microstrain IMUs contain higher performance parts and more internal filtering.

The only trial to break either of these trends was the 1.25 m/s trial, in which the Microstrain IMU had a greater RMSE than the 1.25 m/s BNO IMU, and then the 1.5 m/s Microstrain IMU. Given that this one trial broke both of the otherwise very solid trends, it seems to be an outlier, and there may have been some external factor during this trial that was altering the data received by the Microstrain IMU.

Experiment 3:

Again, the Microstrain IMUs generally outperformed the BNO IMUs in all three metrics: RMSE, phase shift, and phase shift adjusted RMSE.

One important thing to note here is that the right leg trials experienced much greater RMSE values than the left leg trials. Upon inspecting the data, it was found that this was again due to high amounts of force interfering with the IMU performance, as the IMUs were worn on the left leg for every single trial (this caused greater error in the right leg trials because when the right leg moves forward first, the subject is pushing off of their left leg). This can be visually seen in the hip flexion angle graphs.

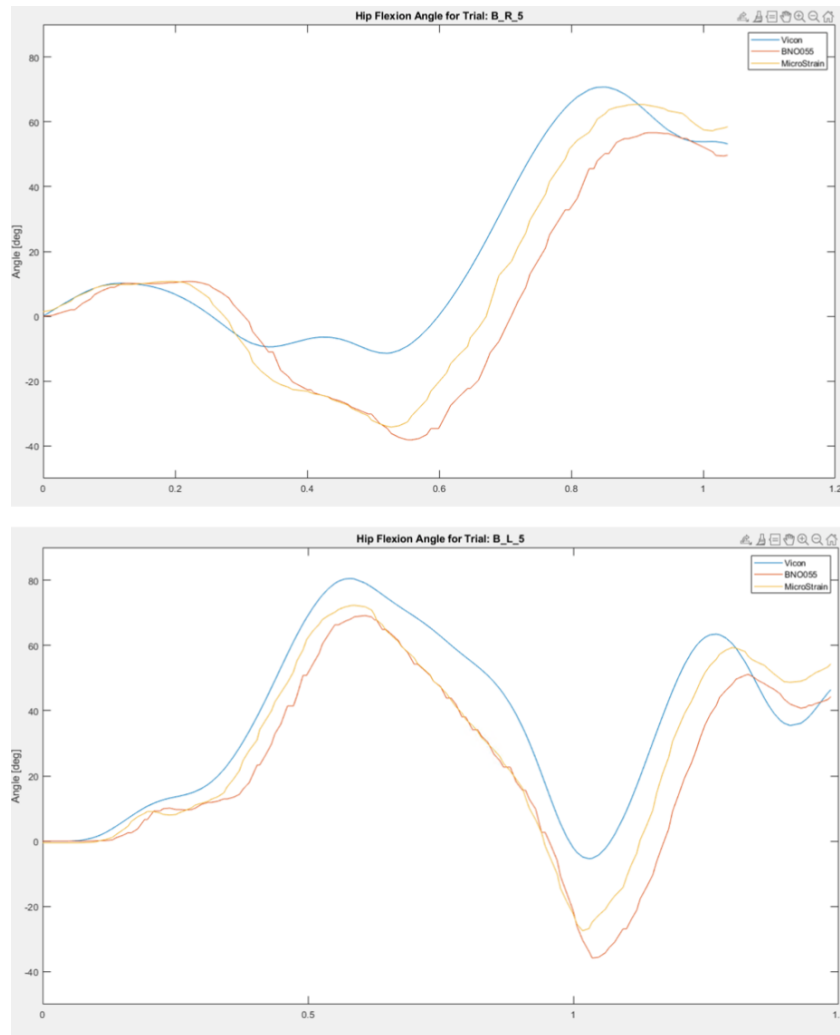


Figure 7. Hip angle flexion comparison between right and left legs.

From the figures, it can be seen that in the right leg trial (top), motion capture reading (blue) wavers upon heel strike, but the Microstrain and BNO IMUs (yellow and orange) do not. This is not observed in the left leg trial (bottom) where the motion capture and IMU readings track the same general trend throughout the whole motion. The reason for this discrepancy is likely that the IMUs were placed on the subject's right leg, so force through the right leg interfered with IMU data collection, whereas force through the left leg did not.

Another unexpected aspect of the data was that phase shifted RMSE did not always produce a lower RMSE than non-shifted RMSE. Shifting the data attempts to line up the peaks and troughs of all of the angle readings, so that angular reading performance can be determined independently of any delays present in the readings. An example of unshifted data (top) and shifted data (bottom) are shown below.

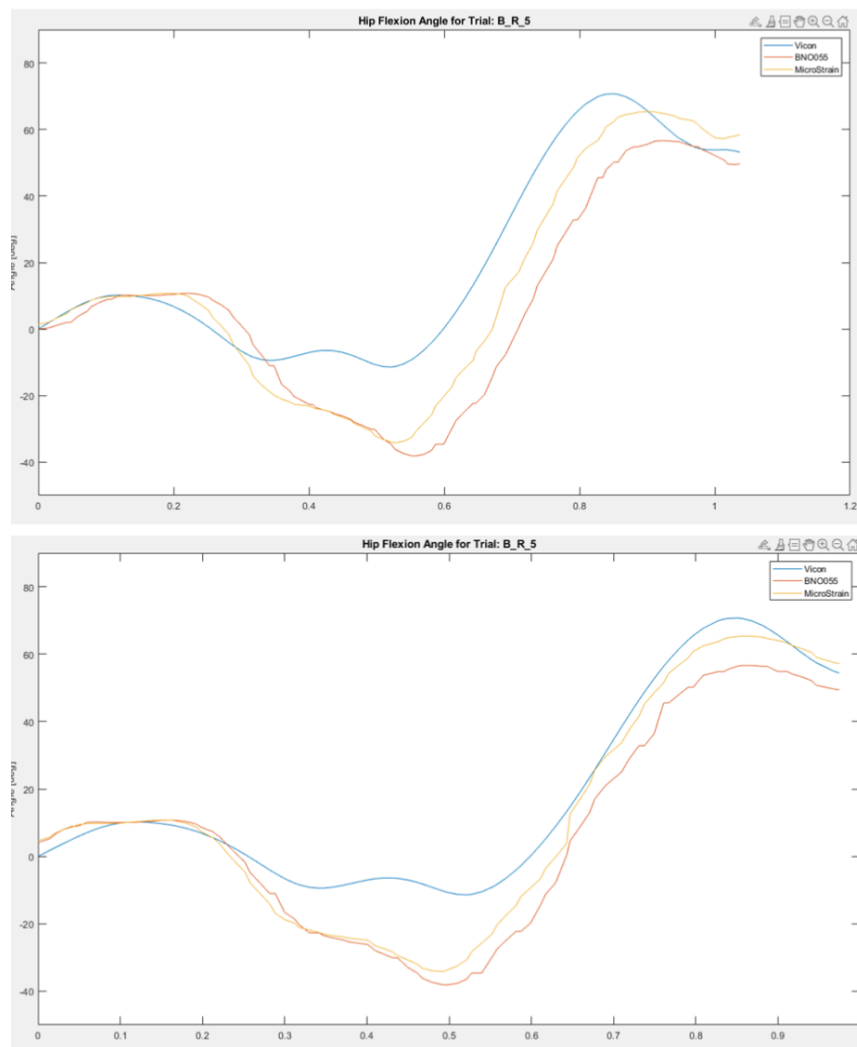


Figure 7. Comparison between shifted and unshifted data.

It should be expected that shifting the data would always lead to a lower RMSE, however this was not the case in many of the trials analyzed. The primary reason

for this phenomenon in the data is likely that in order to line up all of the data, some data points need to be removed at the ends. This likely led to higher RMSE values in shifted data simply because the data generally appears to be more inaccurate in the middle, where peaks and troughs occur. Therefore removing data points from the ends, removes data points that are bringing down the RMSE in a given trial. This theory is supported by the fact that shifting the data seemed to significantly reduce the RMSE in trials with larger phase shifts, but saw diminishing returns as phase shifts decreased.

Conclusion

Two major conclusions can be drawn from this research. The first is that the Microstrain IMUs had higher accuracy in these experiments than the BNO IMUs, although both of them have a large amount of error. The second conclusion is that as a sensor, IMUs are prone to far more error when exposed to greater forces. This puts a limitation on their usefulness in devices that are going to be experiencing large forces.

References

- 1) Mengüç, Y., Park, Y.-L., Pei, H., Vogt, D., Aubin, P. M., Winchell, E., Fluke, L., Stirling, L., Wood, R. J., & Walsh, C. J. (2014). Wearable soft sensing suit for human gait measurement. *The International Journal of Robotics Research*, 33(14), 1748–1764. <https://doi.org/10.1177/0278364914543793>
- 2) T. Nef and R. Riener, "Shoulder actuation mechanisms for arm rehabilitation exoskeletons," 2008 2nd IEEE RAS & EMBS International Conference on Biomedical Robotics and Biomechatronics, Scottsdale, AZ, USA, 2008, pp. 862-868, doi: 10.1109/BIOROB.2008.4762794.

- 3) Shisheie, R. Design, Fabrication, and Control of an Upper Arm Exoskeleton Assistive Robot. <https://doi.org/10.33915/etd.6636>

- 4) Alemi MM, Geissinger J, Simon AA, Chang SE, Asbeck AT. A passive exoskeleton reduces peak and mean EMG during symmetric and asymmetric lifting. *Journal of Electromyography and Kinesiology*. 2019;47:25-34. doi:10.1016/j.jelekin.2019.05.003.

- 5) Abdoli-E, M., Agnew, M. J., & Stevenson, J. M. (2006). An on-body personal lift augmentation device (PLAD) reduces EMG amplitude of erector spinae during lifting tasks. *Clinical Biomechanics*, 21(5), 456–465. <https://doi.org/10.1016/j.clinbiomech.2005.12.021>

- 6) de Looze, M. P., Bosch, T., Krause, F., Stadler, K. S., & O'Sullivan, L. W. (2015). Exoskeletons for industrial application and their potential effects on physical work load. *Ergonomics*, 59(5), 671–681. <https://doi.org/10.1080/00140139.2015.1081988>

- 7) Lee, S., Kim, J., Baker, L., Long, A., Karavas, N., Menard, N., ... Walsh, C. J. (2018). Autonomous multi-joint soft exosuit with augmentation-power-based control parameter tuning reduces energy cost of loaded walking. *Journal of NeuroEngineering and Rehabilitation*, 15(1). <https://doi.org/10.1186/s12984-018-0410-y>

- 8) Iosa, M., Picerno, P., Paolucci, S., & Morone, G. (2016). Wearable inertial sensors for human movement analysis. *Expert review of medical devices*, 13(7), 641–659. <https://doi.org/10.1080/17434440.2016.1198694>

- 9) Ajdaroski, M., Tadakala, R., Nichols, L., & Esquivel, A. (2020). Validation of a device to measure knee joint angles for a dynamic movement. *Sensors*, 20(6), 1747. <https://doi.org/10.3390/s20061747>

Certificate Of Completion

Envelope Id: 0AF987DFFB304F9AB63185B75CFA2421

Status: Completed

Subject: Please DocuSign: Ugrad thesis final draft-5_AM.pdf

Source Envelope:

Document Pages: 22

Signatures: 1

Envelope Originator:

Certificate Pages: 1

Initials: 0

Essy Behraves

AutoNav: Enabled

North Avenue

Envelope Stamping: Disabled

Atlanta, GA 30332

Time Zone: (UTC-05:00) Eastern Time (US & Canada)

ebehnavesh3@gatech.edu

IP Address: 143.215.225.251

Record Tracking

Status: Original

Holder: Essy Behraves

Location: DocuSign

12/10/2021 2:29:57 PM

ebehnavesh3@gatech.edu

Signer Events

Essy Behraves

ebehnavesh3@gatech.edu

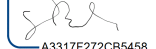
Director of Undergraduate Studies

Georgia Tech

Security Level: Email, Account Authentication (Optional)

Signature

DocuSigned by:

A3317F272CB5458...

Signature Adoption: Uploaded Signature Image

Using IP Address: 143.215.225.251

Timestamp

Sent: 12/10/2021 2:30:45 PM

Viewed: 12/10/2021 2:30:51 PM

Signed: 12/10/2021 2:30:55 PM

Electronic Record and Signature Disclosure:

Not Offered via DocuSign

In Person Signer Events**Signature****Timestamp****Editor Delivery Events****Status****Timestamp****Agent Delivery Events****Status****Timestamp****Intermediary Delivery Events****Status****Timestamp****Certified Delivery Events****Status****Timestamp****Carbon Copy Events****Status****Timestamp**

Ryan Casey

rcasey9@gatech.edu

Georgia Institute of Technology

Security Level: Email, Account Authentication (Optional)

COPIED

Sent: 12/10/2021 2:30:45 PM

Viewed: 12/10/2021 3:11:29 PM

Electronic Record and Signature Disclosure:

Not Offered via DocuSign

Witness Events**Signature****Timestamp****Notary Events****Signature****Timestamp****Envelope Summary Events****Status****Timestamps**

Envelope Sent

Hashed/Encrypted

12/10/2021 2:30:45 PM

Certified Delivered

Security Checked

12/10/2021 2:30:51 PM

Signing Complete

Security Checked

12/10/2021 2:30:55 PM

Completed

Security Checked

12/10/2021 2:30:55 PM

Payment Events**Status****Timestamps**